

RESEARCH ARTICLE

Effect of wind and wave directionality on the structural performance of non-operational offshore wind turbines supported by jackets during hurricanes

Kai Wei¹, Sanjay R. Arwade², Andrew T. Myers¹, Vahid Valamanesh¹ and Weichiang Pang³

¹ Department of Civil and Environmental Engineering, Northeastern University, Boston, Massachusetts 02115, USA

² Department of Civil and Environmental Engineering, University of Massachusetts Amherst, Amherst, Massachusetts 01002, USA

³ Glenn Department of Civil Engineering, Clemson University, Clemson, South Carolina 29634, USA

ABSTRACT

Risk of hurricane damage is an important factor in the development of the offshore wind energy industry in the United States. Hurricane loads on an offshore wind turbine (OWT), namely wind and wave loads, not only exert large structural demands, but also have temporally changing characteristics, especially with respect to their directions. Waves are less susceptible to rapid changes, whereas wind can change its properties over shorter time scales. Misalignment of local winds and ocean waves occurs regularly during a hurricane. The strength capacity of non-axisymmetric structures such as jackets is sensitive to loading direction and misalignment relative to structural orientation. As an example, this work examines the effect of these issues on the extreme loads and structural response of a non-operational OWT during hurricane conditions. The considered OWT is a 5 MW turbine, supported by a jacket structure and located off the Massachusetts coast. A set of 1000 synthetic hurricane events, selected from a catalog simulating 100,000 years of hurricane activity, is used to represent hurricane conditions, and the corresponding wind speeds, wave heights and directions are estimated using empirical, parametric models for each hurricane. The impact of wind and wave directions and structural orientation are quantified through a series of nonlinear static analyses under various assumptions for combining the directions of wind and wave and structural orientation for the considered example structure. Copyright © 2016 John Wiley & Sons, Ltd.

KEYWORDS

offshore wind turbine; hurricane; jacket; directionality; wind-wave misalignment; structural orientation; non-operational; performance

Correspondence

Kai Wei, Department of Civil and Environmental Engineering, Northeastern University, 400 SN, 360 Huntington Ave., Boston, MA 02115, USA.

E-mail: kaiwei.tj@gmail.com

Received 30 October 2015; Revised 25 February 2016; Accepted 1 June 2016

1. INTRODUCTION

Offshore structures located near the U.S. Atlantic coast or in the Gulf of Mexico are exposed to risk of damage from hurricane-induced wind and waves.^{1,2} In the Gulf of Mexico, there are numerous reports of damage and collapse of fixed offshore platforms supported by jacket structures following hurricanes (e.g., Hurricanes Andrew, Lili, Ivan, Katrina, Rita, Gustav and Ike^{3–5}). Near the U.S. Atlantic coast, there are few offshore structures presently; however, this region, which has a rich wind resource, shallow water and proximity to energy demand centers, is expected to be at the center of the emerging offshore wind energy in the U.S..⁶ Although the standards for the design of offshore wind turbines (OWTs) are well established (e.g., IEC 61400-3,⁷ DNV-OS-J101⁸), such standards have been developed primarily for the European offshore environment, a region not exposed to hurricane risk, and thus there are many questions on the validity of directly applying these guidelines to offshore wind structures exposed to hurricane risk. Hurricane-induced wind and waves not only exert large loads on OWTs, but also have significantly varying characteristics over the duration of the hurricane (e.g., the directions of wind and wave).^{2,9,10} Considering hurricane risk in the design of OWTs requires an understanding

of the uncertainties associated with hurricane-induced hazards, wind and wave, and the response of the structure under such conditions. Although the American Bureau of Shipping (ABS) has issued a guideline advising how to consider hurricane-induced loads on OWTs,¹¹ and efforts have been made to adapt the design criteria in API RP 2A-WSD¹² for the design of OWTs exposed to hurricane risk,¹⁰ a comprehensive framework for designing OWTs for hurricane loads has yet to be established.

The effect of wind-wave loading directionality on the ultimate strength capacity, fatigue performance and response frequencies of OWT support structures has been the subject of some attention in the open literature. Li¹³ studied the directional effect of wind and wave loads on OWT jackets using a static pushover procedure and found that (i) the direction of the wind and wave force affects the structure's failure mechanism and ultimate strength capacity significantly and (ii) the largest capacity of the jacket is attained when the jacket is oriented broadside to the dominant wave direction, while the minimum capacity is attained when waves approach at 45° to the sides of the jacket. Philippe *et al.*¹⁴ found through modal analysis that natural modes for a particular floating OWT system are excited differently depending on the approaching direction of the waves. Barj *et al.*¹⁵ examined the impact of wind/wave misalignment on an axisymmetric floating OWT under operational conditions and found that including wind/wave misalignment significantly increases the fatigue damage in the side-to-side direction.

The IEC standard requires that, for design load cases during extreme storms, when the turbine is non-operational, misalignment of the wind and wave directions shall be considered for calculation of the loads acting on the support structure;⁷ however the standard also notes how site-specific measurements allowing for estimation of a joint distribution of wind speed, wave height and their directions are often not available. In addition, the standard does not provide explicit guidance for how to consider a joint distribution of environmental conditions including misalignment in design. During hurricanes, misalignment of local winds and waves occurs regularly because of the curvature of the hurricane wind fields and the hurricane's translation.¹⁶ Based on one observation of the wind and wave field in the Gulf of Mexico during Hurricane Ike, wind directions were found to be counterclockwise relative to the hurricane eye, while the waves in the region in front of the hurricane eye were roughly perpendicular to the local wind direction and the waves in the lower left quadrant of the hurricane eye were nearly opposite to the local wind.¹⁷

In this paper, an analysis framework for assessing hurricane risk to OWTs supported by jackets is developed with particular emphasis on understanding the effect of wind and wave directionality and jacket orientation on structural demands and capacities. The framework combines several simplified empirical models, including Holland's¹⁸ and Young's¹⁹ empirical models to calculate hurricane-induced wind speed and wave height and Moon *et al.*'s model¹⁶ to estimate the wind and wave direction during a hurricane. A numerical example based on simulations using this framework is provided for an OWT supported by a jacket and located off the coast of Massachusetts at the same location as National Oceanic and Atmospheric Administration (NOAA) Buoy #44008. The directionality of the hurricane loads and the effect of this directionality on the performance of the example structure are discussed and the orientation dependence of the structural performance of the example structure is investigated.

2. OVERVIEW OF ANALYSIS FRAMEWORK

In this section, an analysis framework for assessing the performance of OWTs supported by jackets during hurricanes is presented. This framework couples a stochastic hurricane catalog with nonlinear static structural analyses and empirical models for hurricane wind speed, wind direction, wave height and wave direction.

2.1. Analysis configuration and general procedure

Consider an OWT supported by a jacket with orientation defined by the parameters θ_{jacket} and θ_{rotor} and loading direction defined by the parameters θ_{wind} and θ_{wave} , as shown in Figure 1. In this study, true north is defined as the reference axis (i.e., $\theta = 0^\circ$), and all directions are defined as the clockwise angle from the reference axis to the direction of the wind/wave incidence or structural orientation. These four parameters completely define the incident direction of wind and wave relative to the orientation of the jacket and rotor of the OWT. For all analyses considered here, the turbine is modeled as non-operational (i.e., with rotor parked and blades feathered), as would be expected during extreme conditions like a hurricane. The analyses assume perfect yaw control of the non-operational turbine, meaning that the wind direction is always modeled as being normal to the rotor plane and therefore only three parameters are needed to define loading and structural orientation since θ_{rotor} always equals θ_{wind} . A general analysis procedure for assessing the structural performance of a non-operational OWT supported by a jacket during hurricane conditions and including directional effects is provided below:

- (1) Define a hurricane catalog, consisting of parameters defining N hurricane events and reflective of the expected recurrence of hurricanes at a particular site defined by its spatial coordinates (x_0, y_0) . The catalog can consist of historical or synthetic events, depending on the availability of data.

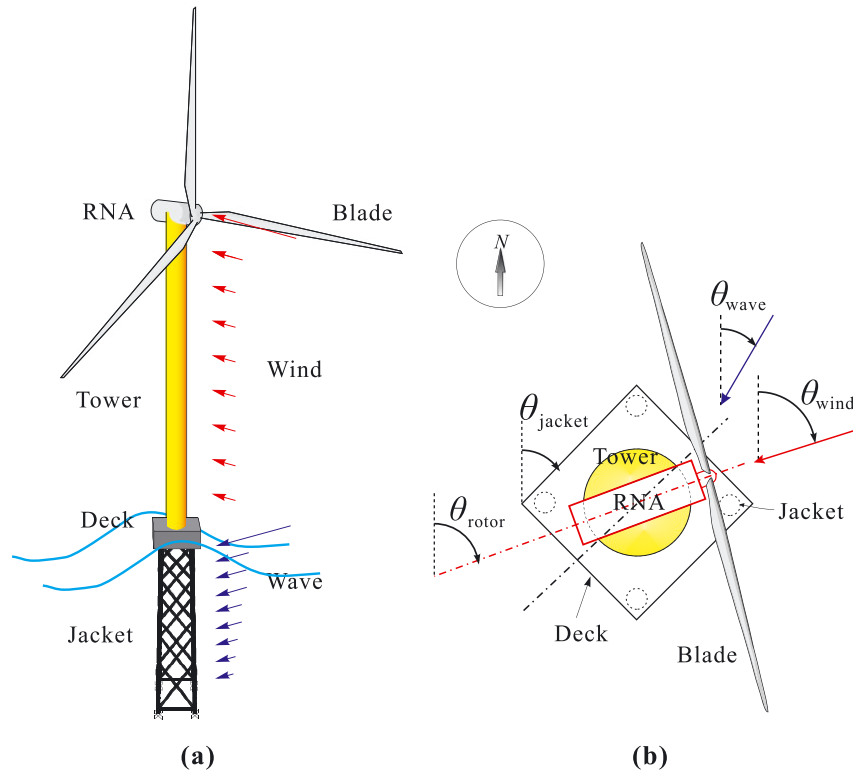


Figure 1. Schematics of (a) a non-operational OWT supported by a jacket subjected to misaligned wind and wave and (b) parameters defining orientations of the structure and loading relative to North (dashed line). In this study it is assumed that $\theta_{rotor} = \theta_{wind}$. RNA = Rotor Nacelle Assembly.

- (2) For every hurricane i in the catalog, calculate time histories of wind speed $V_w(t_i)$, wind direction $\theta_{wind}(t_i)$, significant wave height $H_s(t_i)$ and wave direction $\theta_{wave}(t_i)$ at a particular location.
- (3) From the time histories for the i^{th} event calculated above, find the time t_i^{max} with the maximum significant wave height and determine all wind parameters, $V_w(t_i^{max})$ and $\theta_{wind}(t_i^{max})$, and wave parameters, $H_s(t_i^{max})$ and $\theta_{wave}(t_i^{max})$, at this time. Parameters are selected at the instant of maximum wave. Although wind loading is often the dominant loading for an operational OWT, waves have been found by the authors to be the dominant source of extreme loads for non-operational OWT jackets under similar extreme conditions as considered here,²⁰ when the blades are feathered to reduce aerodynamic loads²¹ and when wave-in-deck forces caused by large waves contacting the deck of the jacket, causing large loads and potential damage.⁴
- (4) Convert the wind and wave conditions from Step 3 into static forces distributed over the height of the jacket and OWT and conduct a static structural analysis on a nonlinear (material and geometric) finite element model of the OWT and jacket with the jacket orientation defined by θ_{jacket} . Evaluate the damage states of this structure for this event based on the response estimated by the nonlinear analysis. Details of this process for the numerical example in this paper are provided in Section 3.1 and by Wei *et al.*²⁰
- (5) Repeat Step 4 for all N events in the hurricane catalog and for multiple values of θ_{jacket} .
- (6) Combine the damage estimates from Step 4 and 5 to estimate the occurrence of damage as a function of θ_{jacket} .

2.2. Synthetic hurricane catalog simulation

One method to estimate metocean hazard is the statistical extrapolation of buoy measurements of wind and wave.^{22,23} For hurricane conditions, this approach is typically not sufficient since the historical record of hurricanes (~150 years) is too short to estimate wind and wave conditions at long mean return periods. Instead, for locations where hurricanes are expected to dominate the wind and wave conditions with long return periods, the variability of hurricane conditions (i.e., variability in hurricane path, fetch, size and intensity) can be more appropriately considered through a stochastic catalog that provides tens of thousands of realizations of one year of potential hurricane activity. Such a catalog aims to represent

hurricane risk at a particular site by simulating tens of thousands of years of potential hurricane activity that is consistent with the historical record and characterizes the hurricane events in terms of geographic and atmospheric parameters.^{24–27}

2.3. Empirical models for hurricane-induced wind speed, wave height and their direction

In this study, empirical models based on statistical analyses of measurements of hurricane-induced wind and wave are used to estimate wind speed, wave height and their directions. While more sophisticated numerical models are available (e.g., SLOSH, ADCIRC, SWAN, etc.),^{26,28,29} empirical models are used here for their simplicity and computational ease.^{16,18,19} In particular, this study uses Holland's model¹⁸ for hurricane-induced wind speed, Young's model¹⁹ for hurricane-induced wave height and Moon *et al.*'s model¹⁶ for wind and wave direction.

Holland's model assumes an axisymmetric structure of the hurricane superimposed with the hurricane's translational speed.³⁰ The tangential wind file is given by the pressure field via cyclostrophic balance and expressed as,

$$V_g(r) = \left\{ \frac{B}{\rho} \left(\frac{R_{\max}}{r} \right)^B (P_n - P_c) \exp \left[- \left(\frac{R_{\max}}{r} \right)^B \right] + \frac{1}{4} (V_{tr} \sin(\theta_{tr}) - r f_c)^2 \right\}^{0.5} + \frac{1}{2} (V_{tr} \sin(\theta_{tr}) - r f_c) \quad (1)$$

where $V_g(r)$ is the 1 min averaged gradient wind speed at a distance r from the eye of the hurricane, B is the Holland parameter, R_{\max} is the radius of maximum wind speed, V_{tr} is hurricane translation speed, θ_{tr} is the angle between hurricane direction and a line connecting the center of the hurricane and a particular site, ρ is air density, P_c is central pressure, P_n is ambient pressure and f_c is Coriolis parameter.³¹ The gradient wind speed is then transformed to surface level winds at an elevation equal to the hub height of the turbine, which for the turbine considered in the numerical example in this study is 90 m. The conversion is expressed as,

$$V_w(r) = C_{g \rightarrow 10} C_{10 \rightarrow 90} V_g(r) \quad (2)$$

where V_w is the hub height wind speed, $C_{g \rightarrow 10}$ is a conversion factor equal to 0.71, used to convert between gradient and 10 m wind speeds based on atmospheric boundary layer theory,³² and $C_{10 \rightarrow 90}$ is a conversion factor equal to 1.30, used to convert between 10 m and 90 m wind speeds based on a wind profile power law with exponent equal to 0.14 representing the effects of wind shear.⁷ This wind shear profile is taken from recommendations in IEC 61400-3,⁷ which, as mentioned previously, does not consider hurricane conditions specifically. Hurricane-specific wind shear profile models (e.g., Frank and Ritchie³³) could represent expected wind shear conditions during hurricanes more accurately.

Young's parametric hurricane wave model predicts the spatial distribution of the significant wave height during a hurricane as a function of three hurricane parameters: the radius to maximum winds R_{max} , the maximum wind speed $V_{w,max}$ and the translation speed V_{tr} . The model calculates an equivalent fetch length to account for the situation where the wave speed is comparable to the forward speed of the hurricane. In such a situation, the winds transfer energy to the waves over an effectively longer duration, and this effect is represented through an extended, equivalent fetch length. Based on the equivalent fetch length, the significant wave height is estimated using a standard JONSWAP fetch-limited growth relationship. Young used these concepts to create a simple model that predicts the spatial distribution of the significant wave height at an instant during a hurricane. Young's equations are summarized below,

$$\frac{gH_s}{V_{w,max}^2} = 0.0016 \sqrt{\frac{gF}{V_{w,max}^2}} \quad (3)$$

where g is acceleration because of gravity and F is the equivalent fetch length in meters and defined as,

$$F = (c_a V_{w,max}^2 + c_b V_{w,max} V_{tr} + c_c V_{tr}^2 + c_d V_{w,max} + c_e V_{tr} + c_f) R' \quad (4)$$

where R' is the effective hurricane radius in meters and defined as,

$$R' = 22.5 \times 10^3 \log R_{\max} - 70.8 \times 10^3. \quad (5)$$

The spatial distribution of the significant wave height H_s is provided by Young through a series of spatial plots. The application of Young's model for this study presents a few challenges. First, some less severe storms in the catalog, which have wind speeds smaller than 20 m/s and translation speed faster than 10 m/s, are outside the validated range of parameters

specified by Young and therefore 17% of the hurricane simulations presented here rely on extrapolation of Young’s model. Second, the domain of the predictions of the spatial distribution of wave height is limited to locations within $8R'$ of the hurricane eye, meaning that wave heights can only be calculated for hurricanes in the catalog with eye locations that pass within $8R'$ of the site. It has, however, been reasoned that sites located at distances greater than $8R'$ from the storm eye can be sensibly neglected from the analysis because the wave heights and wind speeds at these sites will be so low. Third, Young’s model assumes that the hurricane is over deep water, not influenced by land, and has a linear path.

Although one can derive the wind direction from Holland’s model,¹⁸ an empirical model proposed by Moon *et al.*¹⁶ for estimating both wind and wave directions during hurricanes is used in this study for consistency. This model assumes an axisymmetric structure of the wind field and a deep, open ocean without consideration of any influences of coastal boundaries. Figure 2 defines the geometric parameters considered by the model, including the current position of the storm $[x(t), y(t)]$, the position of the storm 6 h prior to the current time $[x(t-6), y(t-6)]$ and the position of the site of interest $[x_0, y_0]$.¹⁶ Referring to Figure 2, the direction of the wind speed θ_{wind} is estimated as,

$$\theta'_{wind} = \begin{cases} \tan^{-1} \left[\frac{y_0 - y(t)}{x_0 - x(t)} \right] + \frac{\pi}{2}, & x_0 \geq x(t) \\ \tan^{-1} \left[\frac{y_0 - y(t)}{x_0 - x(t)} \right] + \frac{3\pi}{2}, & x_0 < x(t) \end{cases} \quad (6)$$

$$\theta_{wind} = \frac{3\pi}{2} - \theta'_{wind}. \quad (7)$$

The direction of the propagation of the dominant wave θ_{wave} depends on the position of storm eye 6 h before and is defined by the following equations,

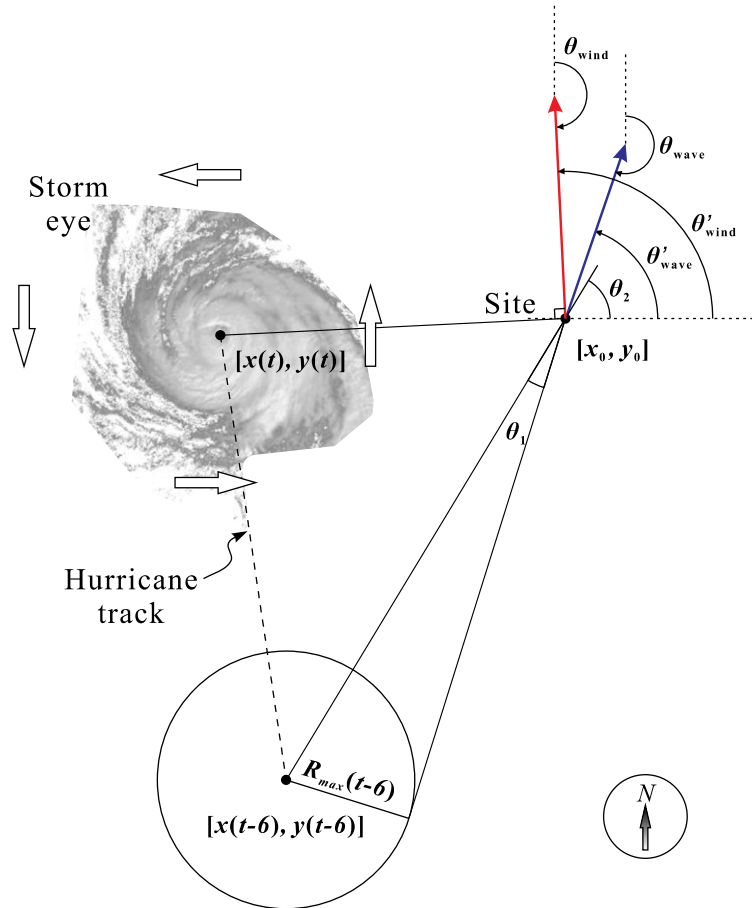


Figure 2. Geometric parameter definition for hurricane generated wind and wave direction model.¹⁶

$$\theta_1 = \sin^{-1} \left[\frac{R_{\max}(t-6)}{\sqrt{[x_0 - x(t-6)]^2 + [y_0 - y(t-6)]^2}} \right] \tag{8}$$

$$\theta_2 = \tan^{-1} \left[\frac{y_0 - y(t-6)}{x_0 - x(t-6)} \right] \tag{9}$$

$$\theta'_{\text{wave}} = \begin{cases} \theta_1 + \frac{\pi}{2}, & x_0 = x(t-6) \\ \theta_1 + (\pi - \theta_2), & x_0 < x(t-6) \\ \theta_1 + \theta_2, & x_0 > x(t-6) \end{cases} \tag{10}$$

$$\theta_{\text{wave}} = \frac{3\pi}{2} - \theta'_{\text{wave}}. \tag{11}$$

An example of the wind and wave direction predicted by Moon *et al.*'s model¹⁶ is illustrated for a synthetic hurricane in Figure 3, which shows that most of the hurricane-induced wind and wave are misaligned, and in some cases the misalignment is as high as 180°.

2.4. Limitations of empirical models

The authors want to emphasize that the empirical models used in this study have many limitations compared to advanced numerical computations, such as coupled ADCIRC-SWAN, SLOSH-SWAN or MIKE21 HD-SW models, especially for near-shore conditions, where OWTs are most likely to be installed and where features not considered by the empirical models, such as coastal terrain and geometry, local bathymetry, tides and currents, and seabed friction, will influence the wind speed, wave height and their directions during hurricanes. Such numerical models were not used here because of (1) the computational demands of running such models for hundreds of hurricane scenarios, (2) inaccessibility of such models to engineers not familiar with numerical modeling of the environment, (3) availability of input data needed to execute such models accurately and (4) ease-of-implementation of parametric, empirical models. Given sufficient computational power and input data availability, considering numerical models for a full stochastic catalog of hurricanes and then developing parametric models for wind speed, wave height and their directions for near-shore, shallow and deep water sites along the U.S. Atlantic coast would be a valuable addition to the literature.

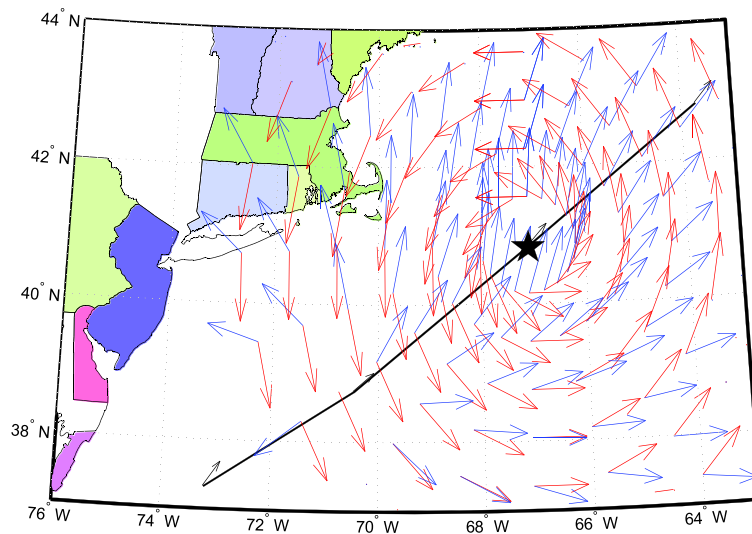


Figure 3. The wind (red arrows) and wave (blue arrows) directions for a synthetic hurricane with eye located near the Massachusetts coast (black solid line—hurricane track; black star—current location of storm eye).

3. NUMERICAL EXAMPLE

In this section, the effect of the direction of hurricane-induced wind and wave on the performance of an OWT is illustrated for a numerical example considering the NREL offshore 5-MW baseline wind turbine³⁴ supported by a jacket designed as part of the UpWind project.³⁵ The site selected for this example is located off the coast of the state of Massachusetts, where NOAA data Buoy #44008 is located (40.502° N 69.247° W). The closest distance from the site to shore is 160 miles.

3.1. Structural model

Schematics of the UpWind jacket and the NREL offshore 5-MW baseline wind turbine are shown in Figure 1. The jacket design consists of four legs with four levels of X-braces and horizontal braces at the bottom. The rotor-nacelle-assembly (RNA) is 90 m above mean sea level, has a total mass of 350,000 kg and is modeled as rigid. The bottom of the 4 m thick concrete deck is 16 m above mean sea level and 66 m above the mudline. The deck has a mass of 666,000 kg and plan dimensions of 9.6 × 9.6 m and is modeled as rigid. The jacket is modeled as fixed at the mudline.

The capacity of the jacket under misaligned wind and wave forces is estimated by nonlinear static structural analyses using the commercial finite element analysis program SAP 2000³⁶ with structural members modeled with Euler–Bernoulli flexural elements and with connections modeled as rigid. Although widely used software packages, such as the program FAST,³⁷ can execute dynamic simulations with coupled aero- and hydrodynamic loading, such packages do not include material nonlinearity resulting from material damage (e.g., yielding). Material nonlinearity is an essential feature to this research, and most programs with robust material nonlinearity (e.g., SAP 2000, USFOS) do not model dynamic structures under coupled aero- and hydrodynamic loads. For these reasons, the analyses considered here are nonlinear static and modeled in SAP 2000. Material nonlinearity is considered through the multiaxial plastic hinge models in SAP 2000,³⁶ with yield stress f_y equal to 380 MPa and hinge rotation at the fully plastic moment equals to $f_y Z L / (6EI)$, where Z is the plastic modulus of the section, L is the hinge length which is equal to 5% of the member length,³⁸ E is the young's modulus and I is the moment of inertia of the section. The yield surface for the hinge, with properties defined in FEMA 356,³⁹ considers interaction of axial force and biaxial bending. Plastic hinges are modeled at the ends of members.

The distribution of loading in the static analysis is determined using separate methods for the aero- and hydrodynamic loads. The aerodynamic loads on the blades, RNA and tower are calculated using the program FAST³⁷ for a steady wind field (i.e., no turbulence) with the effect of wind shear considered with a wind profile power law with exponent equal to 0.14. The model in FAST is rigid with the rotor parked and blades feathered (i.e., non-operational conditions). The hydrodynamic loads on the jacket and deck are calculated for all jacket members based on the kinematics of a single extreme wave calculated at its crest, when the total lateral force per the Morison equation is largest. The kinematics are calculated using the 10th order stream function wave theory. The height of this single extreme wave is equal to $1.86H_s$ ²⁰ and the period of this wave is equal to $11.1\sqrt{H_s/g}$, which is the lower bound of a range of periods specified in the IEC standard,⁷ where g is equal to gravity. The hydrodynamic forces are then calculated from these kinematics according to the Morison equation.⁴⁰ Wave-in-deck force is calculated following API¹² procedure for wave heights that contact the deck.

In this numerical example, performance of the jacket is assessed using three performance levels¹: undamaged,² damaged and³ near collapse. The performance levels are delimited by two damage states¹: first yield of any member in the jacket and² the formation of a plastic collapse mechanism in the jacket. The performance levels here apply only to the jacket support structure and other damage states such as local buckling of the tower, or damage to the blades and electromechanical systems of the nacelle is not considered.

3.2. Hurricane catalog description

Since the historical record of hurricanes at the selected site is short (~150 years), the variability of hurricane conditions (i.e., variability in hurricane path, fetch, size and intensity) is considered through a stochastic catalog that provides tens of thousands of realizations of one year of potential hurricane activity. The stochastic catalog developed at Clemson University for the Atlantic basin by Liu and Pang⁴¹ based on the methodology proposed by Vickery²⁵ is used. In this catalog, the hurricane events are parameterized every six hours in terms of eye position latitude and longitude, central pressure, radius to maximum winds, heading direction, forward translation speed and the Holland B parameter¹⁸ (see Section 2.3 and equation (1) for more details). The numerical examples provided in this section are based on a selection of 1000 hurricanes among 100,000 years of hurricane simulation. The tracks of the selected 1000 hurricane events are illustrated in Figure 4 and are selected from the 100,000 year catalog based on wind speed using Latin hypercube sampling (LHS) such that the 1000 hurricanes approximate the cumulative distribution function of wind speed for the entire catalog at the site where NOAA Buoy #44008 is located. As shown in Figure 4, the majority of the hurricane tracks in the catalog have a strong North-northeast trajectory in the vicinity of the study site. This has implications for the predominant wave direction as shown in later results.

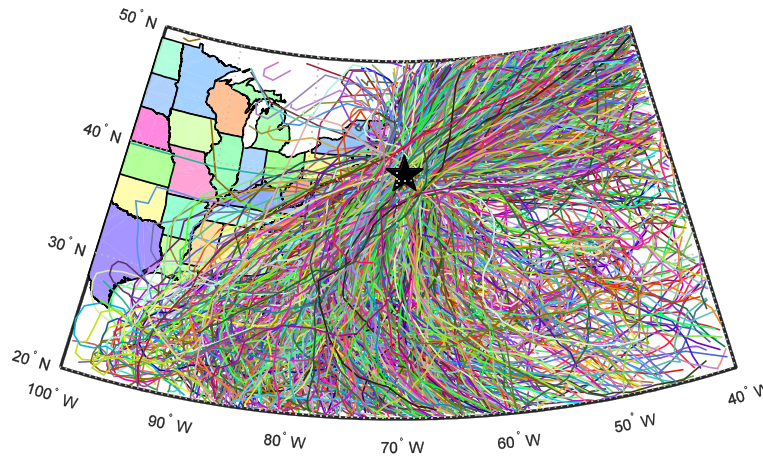


Figure 4. A total of 1000 synthetic hurricane tracks selected from a 100,000 year stochastic catalog.⁴¹ The site of NOAA Buoy #44008 is indicated with a black star.

Of the 1000 hurricane tracks selected for this numerical example, 270 of these tracks do not pass close enough to NOAA Buoy #44008 to be within the spatial domain defined by Young's model. Since the damage to jackets for similar extreme, non-operational conditions has been found by the authors to be dominated by wave loads²⁰ and since locations outside the domain of Young's model are expected to have minimal hurricane-induced waves, it is assumed that these 270 events do not cause damage to the jacket considered in this example. The maximum significant wave height $H_s(t_i^{\max})$ during the duration of hurricane i and the simultaneous 1 min hub height wind speed $V_w(t_i^{\max})$ are plotted in Figure 5 for the 730 effective hurricane tracks for which NOAA Buoy #44008 passes within the domain of Young's model.

It is important to reiterate that the 1000 hurricane tracks considered here have been sampled using LHS to approximate the cumulative distribution function of wind speed from a larger, more comprehensive catalog of hurricane tracks representing 100,000 years of hurricane activity. As such, there is no assurance that these 1000 hurricane tracks will also approximate the cumulative distribution function for wave height; however, as shown in Figure 5, wind speed and wave height are strongly correlated for these 1000 tracks. Assuming this correlation is representative of the entire 100,000 year catalog, the authors also assumed that the differences between the wave distribution from the 1000 tracks and the entire 100,000 year catalog are negligible, and, therefore, that the 1000 tracks, sampled based on wind speed, also approximate the cumulative distribution of wave height.

Estimates of the probability density function (PDF) of the wind direction $\theta_{\text{wind}}(t_i^{\max})$ and wave direction $\theta_{\text{wave}}(t_i^{\max})$ are given in Figure 6. The estimates are obtained from the 730 effective events at the example site. According to Figure 6, the wave direction is concentrated in a range from 180° to 270°, while wind direction is much more broadly distributed.

Figure 7 shows the misalignment between the predictions of wind direction $\theta_{\text{wind}}(t_i^{\max})$ and wave direction $\theta_{\text{wave}}(t_i^{\max})$ at the example site for each of the 730 effective hurricane tracks. Four red lines are superimposed on Figure 7 and these represent contours of constant wind-wave misalignment, $\theta_{\text{wave}}(t_i^{\max}) - \theta_{\text{wind}}(t_i^{\max})$, for misalignments of 0°, 45°, 90° and 135°. Eighty six percent of the 730 effective hurricane tracks have misalignment between 0° and 135°. The mean misalignment is 79° and the standard deviation is 47°.

Figure 8 illustrates the relationship between significant wave height or wind speed and the wind-wave misalignment of all the hurricane tracks. There is no evidence for a significant relationship between wave height or wind speed and misalignment. Figure 8 (a) and (b) look similar because of the strong correlation between wind and wave height (Figure 5).

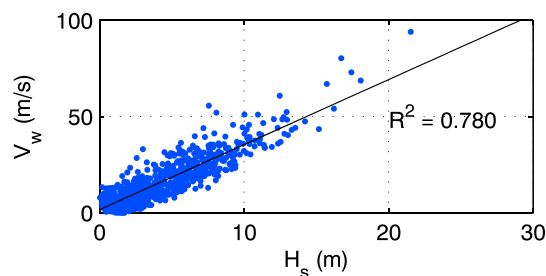


Figure 5. Significant wave height $H_s(t_i^{\max})$ vs. 1 min hub height wind speed $V_w(t_i^{\max})$ for the 730 effective hurricane tracks, where t_i^{\max} is the time at which the maximum wave height of hurricane i occurs.

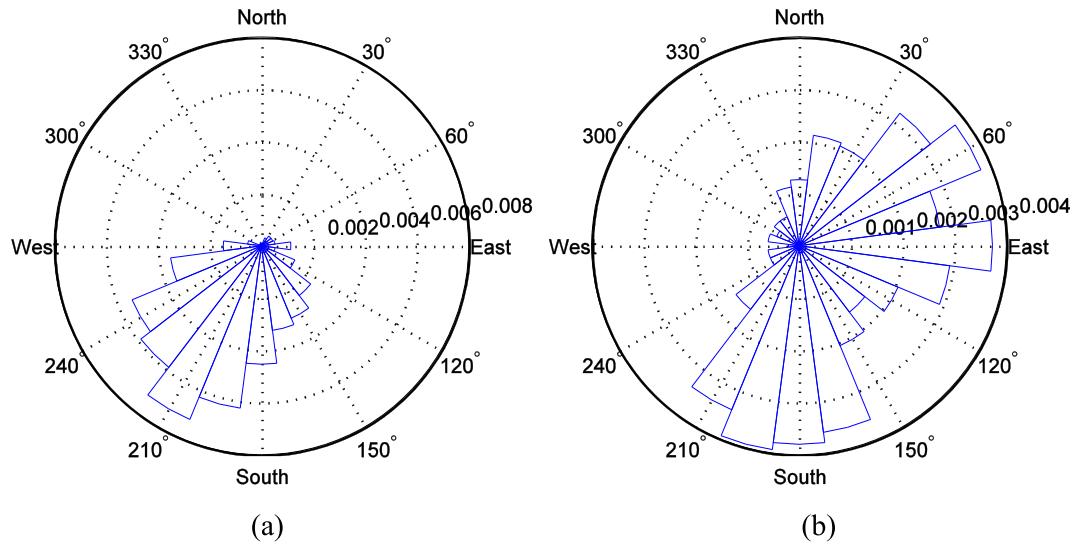


Figure 6. Probability density function (PDF) of most likely (a) wave direction $\theta_{\text{wave}}(t_i^{\text{max}})$ and (b) wind direction $\theta_{\text{wind}}(t_i^{\text{max}})$ estimated from model-based predictions for the synthetic hurricane catalog at Buoy #44008 off the coast of Massachusetts.

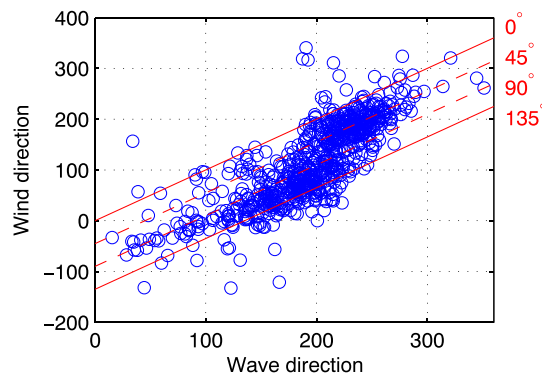


Figure 7. Scatter of the predictions of wave and wind direction for 730 effective hurricane tracks. The red lines show contours of constant wind-wave misalignment, $\theta_{\text{wave}}(t_i^{\text{max}}) - \theta_{\text{wind}}(t_i^{\text{max}})$, for misalignments of 0° , 45° , 90° and 135° .

4. RESULTS AND DISCUSSION OF NUMERICAL EXAMPLE

This section summarizes the results of the considered non-operational OWT supported by a jacket subject to the wind and wave actions generated from the synthetic hurricane catalog. The first part of this section considers five criteria for combining wind and wave directions and assesses the effect of these criteria on the demand (i.e., the resultant base shear) and capacity (i.e., the ultimate lateral strength) of the jacket under wind and wave loading. The second part illustrates the effect of jacket orientation, which is an important preliminary design variable that can influence the probability of structural damage.

4.1. Effect of wind and wave direction and misalignment on structural response

To study the effect of directionality on the demand and capacity of a non-operational OWT jacket, the example structure is assumed to have a fixed orientation $\theta_{\text{jacket}} = 0^\circ$, an orientation in which one of the sides of the square plan of the jacket is perpendicular to true north. For this example structure, five possible criteria for combining wind and wave direction are considered. These five cases are selected to investigate how various assumptions on the alignment of wind and wave influence the demand and capacity of the example structure. The first four cases are simplified approaches and assume that wind and wave directions are aligned (i.e., co-directional). Of these four cases, the first two correspond to the directive in the API specification to assume wind/wave alignment and then consider a range of eight incident loading directions ranging from 0°

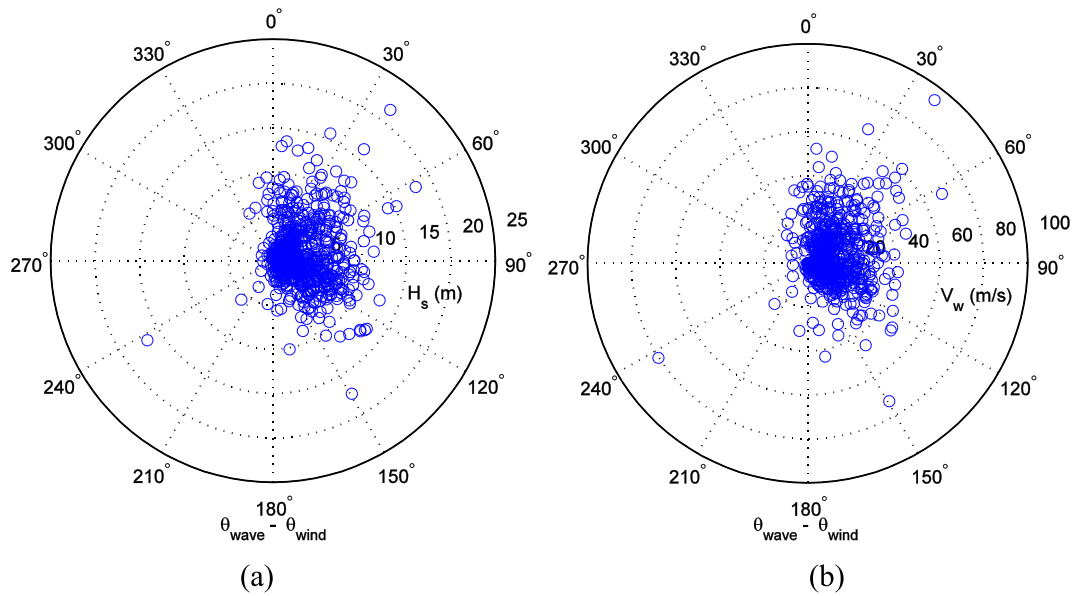


Figure 8. Hurricane wind-wave misalignment plotted as scatter of (a) significant wave height $H_s(t_i^{\max})$ of the hurricane tracks as a function of wind-wave misalignment $\theta_{\text{wave}}(t_i^{\max}) - \theta_{\text{wind}}(t_i^{\max})$ and (b) wind speed $V_w(t_i^{\max})$ of the hurricane tracks as a function of wind-wave misalignment $\theta_{\text{wave}}(t_i^{\max}) - \theta_{\text{wind}}(t_i^{\max})$.

to 315° . For the example structure, which has fourfold rotational symmetry, only two, 0° (Case 1) and 45° (Case 2), of these eight incident loading directions need be considered. The next two cases consider the idea that, if wind or wave dominates the loading, then it may be reasonable to assume that wind and wave are aligned with either the wind direction (Case 3) or the wave direction (Case 4), as estimated individually for each event in the catalog. The final case (Case 5) considers misaligned wind and wave directions, with the directions of both wind and wave estimated individually for each event in the catalog. Of the five cases, this case is the most complicated, but also the most reflective of the estimated conditions. As such, the five considered cases are:

- Case 1: Wind and wave are aligned with $\theta_{\text{wave}} = \theta_{\text{wind}} = 0^\circ$. This is the orientation for which the jacket has the highest capacity.⁴²
- Case 2: Wind and wave are aligned with $\theta_{\text{wave}} = \theta_{\text{wind}} = 45^\circ$. This is the orientation for which the jacket has the lowest capacity.⁴²
- Case 3: Wind and wave are aligned with both wind and wave assumed to come from the direction $\theta_{\text{wind}}(t_i^{\max})$.
- Case 4: Wind and wave are aligned with both wind and wave assumed to come from the direction $\theta_{\text{wave}}(t_i^{\max})$.
- Case 5: Wind and wave are misaligned, with directions $\theta_{\text{wind}}(t_i^{\max})$ and $\theta_{\text{wave}}(t_i^{\max})$, respectively.

Figure 9 shows the resultant base shear demand D_i of the non-operational OWT jacket subjected to $V_w(t_i^{\max})$ and $H_s(t_i^{\max})$ for the five cases of wind and wave alignment defined above. The figure does not show any clear evidence that the wind and wave alignment influences the base shear demand significantly, although for higher wave heights, when wave-in-deck forces occur, the difference between cases can be as high as 7%. Because the calculation of wave forces is based on the Morison equation, which neglects changes to wave kinematics because of interaction with the structure, wave demand on the primary members of the jacket is independent of the wave direction for waves which do not contact the deck. For cases when the wave height is high enough to cause contact the deck, the demand from waves depends on wave direction since the wave-in-deck force depends on the projected frontal area of the deck in the loading direction and the drag coefficient of the deck, both of which depend on the loading direction. For this reason, the differences between the resultant base shear demand is basically negligible for wave heights that do not contact the deck.

The capacity of the structure is sensitive to the loading direction relative to the structural orientation. The first yielding capacity $C_{1,i}$ and plastic mechanism formation capacity $C_{2,i}$ of the example OWT jacket subjected to $V_w(t_i^{\max})$ and $H_s(t_i^{\max})$ are assessed with a nonlinear static analysis to study the effect of loading direction and misalignment on the performance of the structure. The performance of the structure under the i^{th} event is evaluated by equation (12) and the results are plotted in Figure 10, which shows structural performance for the five cases of wind and wave alignment in terms of the following three performance levels:

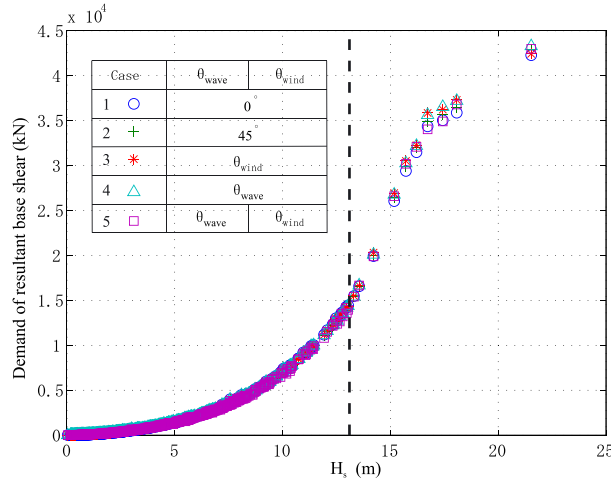


Figure 9. Resultant base shear demand of OWT jacket ($\theta_{\text{jacket}} = 0^\circ$) for the i^{th} hurricane event as a function of significant wave height H_s . The vertical black dashed line indicates the H_s when the wave first contacts the deck.

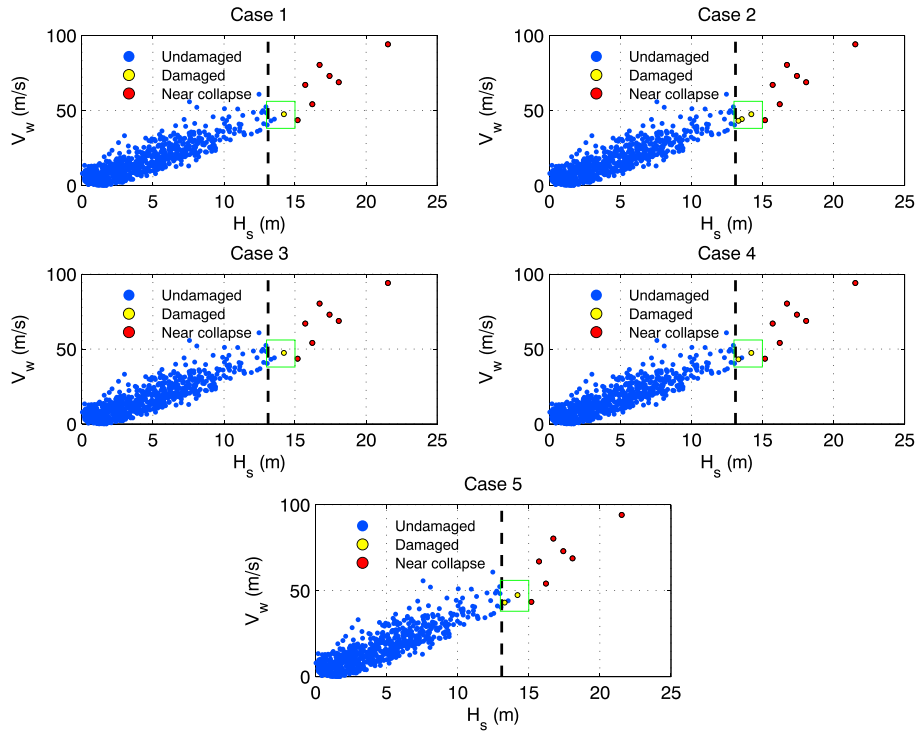


Figure 10. Performance of OWT jacket with $\theta_{\text{jacket}} = 0^\circ$ for five different cases for combining directions of wind and wave loads. The vertical black dashed line indicates the H_s when the wave first contacts the deck.

$$\text{Performance level} = \begin{cases} \text{undamaged,} & C_{1,i} > D_i \\ \text{damaged,} & C_{2,i} > D_i \geq C_{1,i} \\ \text{near collapse,} & C_{2,i} \leq D_i \end{cases} \quad (12)$$

According to Figure 10, all events with wave heights that do not contact the deck (i.e., the event on the left side of the vertical black dashed line) result in an undamaged performance level. The events that cause the near collapse performance level are the same regardless of the loading case, but the events causing the damaged performance level are sensitive to the

loading case. To illustrate this observation, the events resulting in the damaged performance level are highlighted with a green rectangle for each of the five loading cases. The results show that Case 1, which has the strongest capacity, has only 1 event resulting in the damaged performance level, Case 2, having the weakest capacity, has 3, Case 3 has 1, Case 4 has 2 and Case 5 has 2. As such, Case 2 predicts the worst structural performance, while Case 1 and 3 predict the best. In other words, the results for aligned wind and wave with the direction equal to $\theta_{\text{wave}}(t_i^{\text{max}})$ (Case 4) are the same as those for misaligned wind and wave loading (Case 5).

To have a clear view of the relationship between structural performance and wind/wave direction, Figure 11 illustrates the performance level results for Case 5 plotted in directional polar graphs for wave and wind intensities, separately. As shown in Figure 11 (a), there is a clear relationship between wave height and structural performance, with larger wave heights always causing equivalent or worse performance than lower wave heights. Moreover, it is only wave heights large enough to contact the deck (see dashed red circle in Figure 11 (a)), which cause performance levels of damaged or near collapse. There are, however, a few instances, for all cases except Case 2, where wave heights are large enough to contact the deck, but the performance level remains undamaged. The relationship between wind speed and performance is not as clear for wind speed, with conditions associated with larger wind speeds sometimes causing less damage than those associated with higher wind speeds, as shown in Figure 11 (b). As such, for these analyses on a non-operational turbine during hurricane conditions, wave height is a more reliable predictor of damage than wind speed, suggesting that wave loading, particularly wave loading that contacts the deck, is more dominant than wind in causing damage.

4.2. Effect of jacket orientation on structural performance

In the above sections, all results are provided for constant jacket orientation, $\theta_{\text{jacket}} = 0^\circ$. In this subsection, the effect of jacket orientation, which is an important preliminary design variable that can influence the probability of structural damage, is considered. Figure 12 shows the performance of the jacket considered in the numerical example for eight structural orientations, including $0^\circ, 15^\circ, 30^\circ, 45^\circ, 60^\circ, 75^\circ, 90^\circ$ and 105° . The results in the figure are provided for Case 5 where wind and wave are treated as misaligned according to the Moon *et al.* model¹⁶ given in Section 2.3. Considering orientations between 0° and 75° , the performance is shown to vary with structural orientation, with orientations between 15° and 30° (i.e., the alignment of the strong axis of the jacket with the prevailing wave direction, see Figure 6) resulting in the best performance and with an orientation of 75° (i.e., the alignment of the weak axis of the jacket with the prevailing wave direction) resulting in the worst performance. The relationship between performance and jacket orientation is shown to be periodic with a period of 90° , as orientations offset by 90° (e.g., 0° and 90° or 15° and 105°) have identical performance.

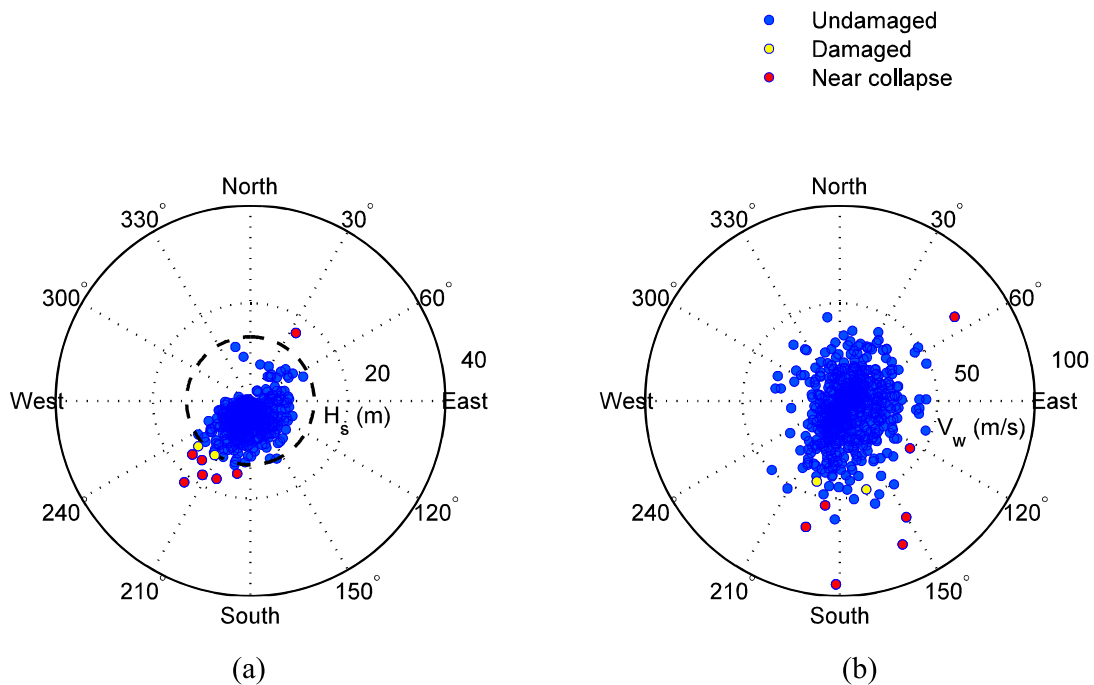


Figure 11. Scatter plots illustrating OWT jacket ($\theta_{\text{jacket}} = 0^\circ$) performance for Case 5, misaligned wave and wind conditions, as a function of (a) significant wave height and wave direction and (b) wind speed and wind direction. Black dashed line in (a) indicates the H_s when the wave first contacts the deck.

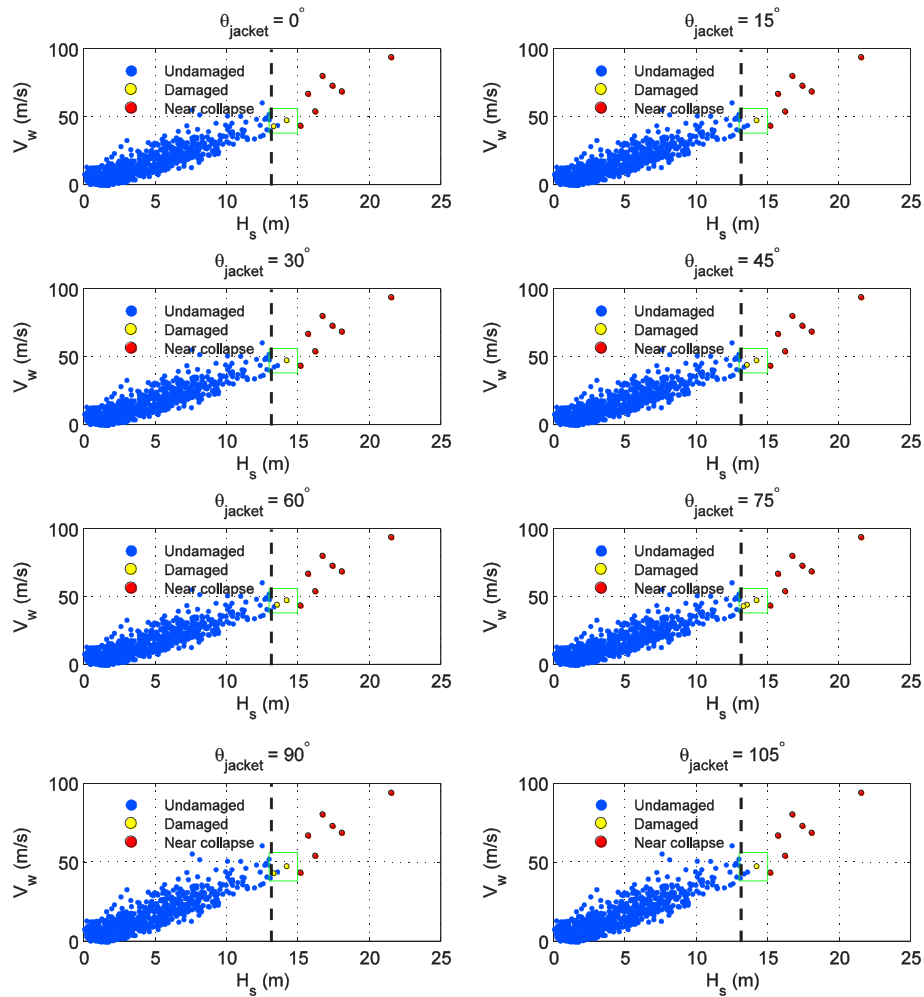


Figure 12. Performance of OWT jacket with eight different orientations ($\theta_{\text{jacket}} = 0^\circ, 15^\circ, 30^\circ, 45^\circ, 60^\circ, 75^\circ, 90^\circ$ and 115°) for Case 5, misaligned hurricane wind-wave conditions. The vertical black dashed line indicates the H_s when the wave first contacts the deck.

5. CONCLUSIONS

This paper has presented a computationally efficient approach to assess the performance of non-operational OWTs supported by jackets under hurricane-induced extreme wind and wave loads including effects of wind and wave direction. Hurricane-induced wind speed and wave height and their directions are calculated based on parametric empirical models that depend on the hurricane eye location, central pressure, maximum wind speed, radius to maximum winds, heading direction, forward translation speed and the Holland B parameter.¹⁸ Three performance levels ranging from undamaged to near collapse are assessed using nonlinear static analysis of the structure for hundreds of synthetic hurricane events within a catalog designed to characterize potential hurricane activity in the future. The approach allows structural performance assessment of OWTs subjected to directional wind and wave loads. Example analyses are conducted for an OWT supported by a four-leg jacket designed as part of the European Union UpWind Project. The example structure is located off the coast of Massachusetts. The major findings of the present study can be summarized as follows:

- The wind-wave misalignments of hurricane-induced wind and wave at the Massachusetts coast are mostly within the range of 0° to 135° .
- The effect of hurricane extreme wind and wave direction (either misaligned or aligned) has less than 10% influence on the resultant base shear demand and has a modest effect on structural performance. Analyses of the example structure for aligned wind and wave coming from the wave direction $\theta_{\text{wave}}(t_i^{\text{max}})$ give the same prediction of performance as analyses for misaligned wind and wave conditions. All else being equal, the loading is most damaging when the loading is coming from a 45° diagonal direction relative to the square plan of the jacket.

- There is a clear relationship between wave height and structural performance, with larger wave heights always causing equivalent or worse performance than lower wave heights. Indeed, it is only wave heights large enough to contact the deck which cause damage. Wave-in-deck forces are found to be a dominant factor in structural performance during hurricanes. It is common design practice not to allow wave-in-deck forces in non-hurricane regions. It might be worth, even for large hurricane induced waves, sticking to this principle.
- For a given hurricane catalog, structural performance is found to be a 90° periodic function of structural orientation for the four-leg example jacket.

Finally, it is emphasized that the present findings are for a given structure with a hypothetical location near the Massachusetts coast, and the finding that the influence of directionality is modest may not apply for all kinds of offshore conditions during hurricanes. Nevertheless, the current findings indicate that directionality may not be a significant factor in determining structural performance and that a simplified approach of assuming wind and wave to be co-directional and incident from the weak axis of the structure may result in only modest design conservatism and a greatly simplified analysis procedure.

ACKNOWLEDGEMENT

This material is based upon work supported by the National Science Foundation under Grant Nos. CMMI-1234560 and CMMI-1234656, the Massachusetts Clean Energy Center, the University of Massachusetts at Amherst and Northeastern University. Any opinions, findings and conclusions expressed in this material are those of the authors and do not necessarily reflect the views of the National Science Foundation or other sponsors.

REFERENCES

1. Wang DW, Mitchell DA, Teague WJ, Jarosz E, Hulbert MS. Extreme waves under Hurricane Ivan. *Science* 2005; **309**: 896.
2. Sparks PR. Wind speeds in tropical cyclones and associated insurance losses. *Journal of Wind Engineering and Industrial Aerodynamics* 2003; **91**: 1731–1751.
3. Spong RE, Puskar F. Assessment of Fixed Offshore Platform Performance in Hurricanes Andrew, Lili and Ivan. *Energo Engineering Inc.*, 2005.
4. Puskar F, Verret S. Assessment of Fixed Offshore Platform Performance in Hurricanes Katrina and Rita. *Energo Engineering Inc.*, 2007.
5. Energo Engineering Inc. Assessment of Damage and Failure Mechanisms for Offshore Structures and Pipelines In Hurricanes Gustav And Ike, 2010.
6. Dvorak MJ, Corcoran BA, Ten Hoeve JE, McIntyre NG, Jacobson MZ. US East Coast offshore wind energy resources and their relationship to peak-time electricity demand. *Wind Energy* 2013; **16**: 977–997.
7. International Electrotechnical Commission. Wind Turbines—Part 3: Design Requirements for Offshore Wind Turbines, IEC 61400-3, 2009.
8. Det Norske Veritas. Design of Offshore Wind Turbine Structures. *DNV-OS-J101*, 2004.
9. Cruz AM, Krausmann E. Damage to offshore oil and gas facilities following hurricanes Katrina and Rita: an overview. *Journal of Loss Prevention in the Process Industries* 2008; **21**: 620–626.
10. Rose S, Jaramillo P, Small MJ, Grossmann I, Apt J. Quantifying the hurricane risk to offshore wind turbines. *Proceedings of the National Academy of Sciences* 2012; **109**: 3247–3252.
11. American Bureau of Shipping. Design Standards for Offshore Wind Farms, 2011.
12. API R. Recommended Practice for Planning, Designing, and Constructing Fixed Offshore Platforms-Working Stress Design. *API RP 2A-WSD 21st Edition*, 2005.
13. Li P. Analysis and Design of Offshore Jacket Wind Turbine. *Master Thesis, Department of Marine Technology, Norwegian University of Science and Technology*, 2010.
14. Philippe M, Babarit A, Ferrant P. Modes of response of an offshore wind turbine with directional wind and waves. *Renewable Energy* 2013; **49**: 151–155.
15. Barj L, Stewart S, Stewart G, Lackner M, Jonkman J, Robertson A, Matha D. Wind/Wave misalignment in the loads analysis of a floating offshore wind turbine, 2014.

16. Moon IJ, Ginis I, Hara T, Tolman HL, Wright CW, Walsh EJ. Numerical simulation of sea surface directional wave spectra under hurricane wind forcing. *Journal of Physical Oceanography* 2003; **33**: 1680–1706.
17. Hu K, Chen Q. Directional spectra of hurricane-generated waves in the Gulf of Mexico. *Geophysical Research Letters* 2011; **38**: L19608.
18. Holland GJ. An analytic model of the wind and pressure profiles in hurricanes. *Monthly Weather Review* 1980; **108**: 1212–1218.
19. Young IR. Parametric hurricane wave prediction model. *Journal of Waterway Port Coastal and Ocean Engineering-Asce* 1988; **114**: 637–652.
20. Wei K, Arwade SR, Myers AT. Incremental wind-wave analysis of the structural capacity of offshore wind turbine support structures under extreme loading. *Engineering Structures* 2014; **79**: 58–69.
21. Li Q, Gao Z, and Moan T. Extreme response analysis for a jacket-type offshore wind turbine using environmental contour method. In *Safety, Reliability, Risk and Life-Cycle Performance of Structures and Infrastructures*. CRC Press: New York, NY, 2014; 5597–5604.
22. Zachary S, Feld G, Ward G, Wolfram J. Multivariate extrapolation in the offshore environment. *Applied Ocean Research* 1998; **20**: 273–295.
23. Soukissian TH. Probabilistic modeling of directional and linear characteristics of wind and sea states. *Ocean Engineering* 2014; **91**: 91–110.
24. Li Y, Ellingwood BR. Hurricane damage to residential construction in the US: importance of uncertainty modeling in risk assessment. *Engineering Structures* 2006; **28**: 1009–1018.
25. Vickery P, Skerlj P, Twisdale L. Simulation of hurricane risk in the U.S. using empirical track model. *Journal of Structural Engineering* 2000; **126**: 1222–1237.
26. Pei B, Pang W, Testik F, Ravichandran N, Liu F. Mapping joint hurricane wind and surge hazards for Charleston, South Carolina. *Natural Hazards* 2014; **74**: 1–29.
27. Hallegatte S. The use of synthetic hurricane tracks in risk analysis and climate change damage assessment. *Journal of Applied Meteorology and Climatology* 2007; **46**: 1956–1966.
28. Dietrich JC, Zijlema M, Westerink JJ, Holthuijsen LH, Dawson C, Luettich RA, Jensen RE, Smith JM, Stelling GS, Stone GW. Modeling hurricane waves and storm surge using integrally-coupled, scalable computations. *Coastal Engineering* 2011; **58**: 45–65.
29. Strauss D, Mirferendesk H, Tomlinson R. Comparison of two wave models for Gold Coast, Australia. *Journal of Coastal Research* 2007; **SI 50**: 312–316.
30. Bao S, Xie L, Pietrafesa LJ. An asymmetric hurricane wind model for storm surge and wave forecasting. *27th Conference on Hurricanes and Tropical Meteorology*, 2006.
31. Xie L, Bao S, Pietrafesa LJ, Foley K, Fuentes M. A real-time hurricane surface wind forecasting model: formulation and verification. *Monthly Weather Review* 2006; **134**: 1355–1370.
32. Powell MD, Vickery PJ, Reinhold TA. Reduced drag coefficient for high wind speeds in tropical cyclones. *Nature* 2003; **422**: 279–283.
33. Frank WM, Ritchie EA. Effects of vertical wind shear on the intensity and structure of numerically simulated hurricanes. *Monthly Weather Review* 2001; **129**: 2249–2269.
34. Jonkman JM, Butterfield S, Musial W, Scott G. Definition of a 5-MW reference wind turbine for offshore system development, 2009.
35. Vemula NK, DeVries W, Fischer T, Cordle A, Schmidt B. Design solution for the upwind reference offshore support structure. *Upwind deliverable D4.2.5*, 2010.
36. CSI. SAP2000: Integrated Finite Element Analysis and Design of Structures, 1997.
37. Jonkman JM, Buhl Jr ML. FAST user's guide, 2005.
38. Chen W-F, Sohal I. *Plastic Design and Second-Order Analysis of Steel Frames*. Springer-Verlag: New York, 1995.
39. Building Seismic Safety Council (U.S.). Prestandard and commentary for the seismic rehabilitation of buildings. *Report FEMA-356*, Washington, DC, 2000.
40. Morison JR, O'Brien MP, Johnson JW, Schaaf SA. The force exerted by surface waves on piles. *Journal of Petroleum Technology* 1950; **2**: 149–154.
41. Liu F, Pang W. Influence of climate change on future hurricane wind hazards along the US eastern coast and the gulf of Mexico. In *Advances in Hurricane Engineering*. ASCE: Miami, FL, 2012; 573–584.
42. Wei K, Arwade SR, Myers AT, Valamanesh V. Directional effects on the reliability of non-axisymmetric support structures for offshore wind turbines under extreme wind and wave loadings. *Engineering Structures* 2016; **106**: 68–79.